Finite element modeling and simulation of a microstructure silicon beam resonant

Mohamed Shaglouf[1*], ElJaroshi Diryak[2] ,Ahmed Abugalia[3]

shaglouf@SU.edu.ly, aljaroshi1966@gmail.com,abugaliass@su.edu.ly

1,2,3 Department of Electrical and Electronics, College of Engineering, Sirte University, Libya

A B S T R A C T

This paper establishes the Finite Element Method (FEM) model of a practical silicon beam resonator attached to a diaphragm used for measuring pressure. In this paper presents two location error models. Analyze, calculate, and investigate the relationship between the basic natural frequency of the beam resonator and the measured pressure for two error models are discussed.

Key Words: Finite Element Method, Beam, Pressure.

1 Introduction

During the past decade, many experts in sensor technology have noticed the rapid development in silicon resonant sensors. The silicon microstructure resonant sensors are noted for the advantages of a generalized resonant sensor, such as direct digital output (without A/D conversion), long-term stability, low hysteretic and high repeatability. Other advantages of silicon material are excellent mechanical properties; high strength; free from mechanical hysteretic; suit ability to batch processing at low cost; and the compatibility of mechanical and electrical properties. Meanwhile, the dynamic characteristics of silicon resonant sensors are much better than those of conventional ones, due to their high working frequency [1]. In addition, the temperature characteristics of silicon resonant sensors are much better than those of another important silicon sensors such as the piezoresistive sensor. It is much easier to interface them with a microprocessor to develop smart or 'intelligent' sensors or sensor systems due to their unique operating principle based on the relationship between the natural frequency and measured signal instead of the silicon piezoresistive effect. Recently, it has been reported that some prototypes, with different structure and configurations, and even few batch products of silicon resonant sensors have come into being for measuring pressure, differential pressure or force. They have been developed and manufactured in Japan, USA, Netherlands and Britain. Although the properties of these silicon resonant sensors have not reached the designed criteria, they could be used widely in many technical fields in the near future.

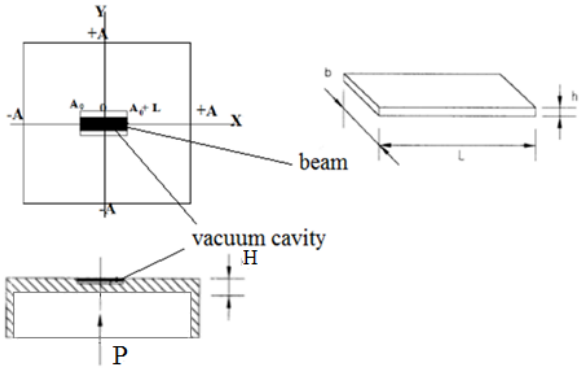

Figure 1: *Sensing structure of the sensor.*

Figure 1 shows the structure of a silicon resonant sensor for measuring pressure. The preliminary sensing unit is a square diaphragm. The measured pressure acts perpendicularly to the lower surface of the diaphragm and yields the stress. T]he final sensing unit is a beam, which is attached to the upper surface of the diaphragm. Moreover, the thickness of the beam h should be less than the thickness of the diaphragm H, and the width of the beam L should be less than the half length of the diaphragm A. Based on the above structural feature, an appropriate initial stress is applied along the axial direction of the beam, which is almost identical with the stress of the square diaphragm at the same position. Thus the natural frequency of the beam is varied with the applied pressure which acts on the square diaphragm. Therefore, the pressure will be measured by the natural frequency changes of the beam. In addition, the beam resonator has a very high Q factor because it can be packaged within a vacuum housing.

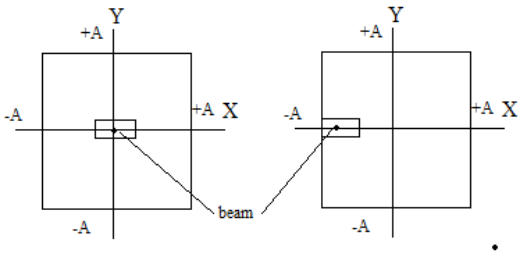

Figure 2: *Ideal locations of the beam at the diaphragm.*

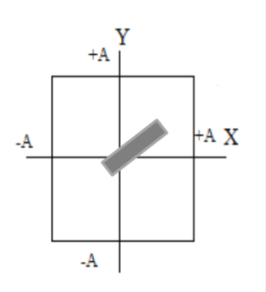

Figure 3: *Error model 1 of beam's location at the diaphragm*

Figure 2 shows the ideal location scheme of the beam. Figure 3 shows the location error model 1 within the positive stress range, while Figure 4 shows the location error model 2 within the negative stress range. It is certain that the frequency-pressure relationship varies with the deviation B in the x-axis, deviation D in the y-axis and the angular deviation a relative to its ideal location for the above error cases. In order to improve the exchangeability of the sensor, it is necessary to investigate the influence laws of the above deviations on the frequency-pressure relationship of the beam resonator. The objective of this paper is to study the above problems in order to obtain some directions during developing the silicon resonator sensors by using of a finite element model (FEM).

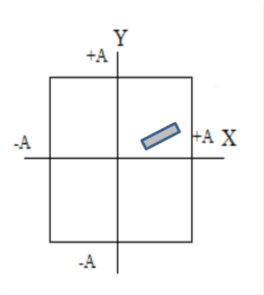

Figure 4: *Error model 2 of beam's location at the diaphragm*

2 Stresses on the upper surface of the square diaphragm

According to the structural feature and the design demands for the sensor, the square diaphragm is within the range of a small deflection. Then the differential equation can be written as follows:

$$\frac{\partial^4 W(x,y)}{\partial x^4} + 2\frac{\partial^4 W(x,y)}{\partial x^2 \partial y^2} + \frac{\partial^4 W(x,y)}{\partial y^4} = \frac{P}{D_s} \tag{1}$$

$$\text{Where } D_s = \frac{EH^3}{12(1-\mu^2)}$$

Where W (x,y) is the displacement of the square diaphragm under the applied pressure P, and Ds is the flexural rigidity of the square diaphragm.

And according to the built-in edge of the square diaphragm, its displacement can be assumed as follows:

$$W(x,y) = W_{\max} H\left(\frac{x^2}{A^2} - 1\right)^2 \left(\frac{y^2}{A^2} - 1\right)^2 \tag{2}$$

Where Wmax is the ratio between the maximum normal displacement and the thickness of the square diaphragm, and A, H are the half-length and thickness of the square diaphragm.

By substituting Eq. (2) into Eq. (1), the displacement, W(x,y) can be obtained. Then stresses on the upper surface of the square diaphragm can be also obtained.

$$\rho_x(x,y)=-\frac{49p}{96}\left(\frac{A}{H}\right)^2\left[\left(\frac{3x^2}{A^2}-1\right)\left(\frac{y^2}{A^2}-1\right)^2+\mu\left(\frac{x^2}{A^2}-1\right)^2\left(\frac{3y^2}{A^2}-1\right)\right]$$
$$\rho_y(x,y)=-\frac{49p}{96}\left(\frac{A}{H}\right)^2\left[\left(\frac{3y^2}{A^2}-1\right)\left(\frac{y^2}{A^2}-1\right)^2+\mu\left(\frac{y^2}{A^2}-1\right)^2\left(\frac{3x^2}{A^2}-1\right)\right] \quad (3)$$

Where σx(x,y),σy(x,y) Stresses of the square diaphragm.

3 Finite element model of the beam

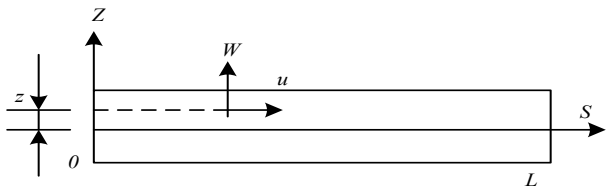

Figure 5: *Mathematical model of the beam*

Figure 5 shows the mathematical model of the beam. The vibrating displacements of the beam at an arbitrary point are as follows:

$$\begin{cases} u(s,z,t) = -z\dfrac{dw(s)}{ds}\cos\omega t \\ w(s,t) = w(s)\cos\omega t \end{cases} \quad (4)$$

Where u (s,z,t)-w (s,t) are axial and normal vibrating displacements of the beam in Cartesian coordinate of the beam, and s ,z are axial and normal coordinates of the beam in Cartesian coordinate of the beam.

The energy expressions of the beam resonator can be written as follows:

The potential energy

$$U=\frac{Ebh^3\cos^2\omega t}{24}\int_S\left[\frac{d^2w(s)}{ds^2}\right]^2 ds \quad (5)$$

Where, U is the potential energy of the beam ,and S is the integrated length of the beam.

The kinetic energy

$$T=\frac{\rho bh\omega^2\sin^2\omega t}{2}\int_S\left[w(s)\right]^2 ds \quad (6)$$

Where, T is the kinetic energy of the beam, and ρ is the density of the sensing structure.

In addition, the initial potential energy of the beam, which is caused by $\sigma_s^0(s)$, is

$$U_0 = -\frac{bh\cos^2 \omega t}{2}\int_S \sigma_s^0(s)\left[\frac{dw(s)}{ds}\right]^2 ds \qquad (7)$$

From Fig(1) and equation (3), according to the above analyses,

$$\sigma_s^0(s) = \sigma_x(x,0) = \frac{49P}{96}\left(\frac{A}{H}\right)^2\left[\left(\frac{3x^2}{A^2}-1\right)-\mu\left(\frac{x^2}{A^2}-1\right)^2\right] \qquad (8)$$

Where σ_s^0 (s) is the initial axial stress of the beam.

The following relation for the error cases yields:

$$\sigma_s^0(s) = \sin^2\beta(s)\sigma_x(x,y)+\cos^2\beta(s)\sigma_y(x,y) \qquad (9)$$

Then the total potential energy of the beam is:

$$U_T = U - U_0 \qquad (10)$$

Where U0 is the initial potential energy of the beam, which is caused by σ_s^0 (s) ,and UT is the total potential energy of the beam.

In Eq. (7), if σ_s^0 (s) is a constant σ_s^0 the analytic relationship between the basic natural frequency and the initial axial stress can be directly obtained:

$$\omega = \frac{22.38h}{L^2}\sqrt{\frac{E}{12\sigma}}\sqrt{1+0.295\frac{\sigma_s^0 L^2}{Eh^2}} \qquad (11)$$

Where ω[rad/s],w(s) Natural frequency and its corresponding vibrating shape along the axial direction of the beam.

However, from Eqs. (3), (8) and (9), $\sigma_s^0(s)$ is varying. Therefore, The finite element equation of the beam resonator can be written as follows:

$$\left(\boldsymbol{K}-\omega^2\boldsymbol{M}\right)\boldsymbol{a}=0 \qquad (12)$$

Where K is assembly stiffness Matrix, M-assembly is Mass Matrix, and a is the assembly nodal vector, consisting of all aj.

For the actual structural features of Fig. 1, the boundary conditions of the beam are as follows

$$\begin{cases} s = -a: & w(s) = w^{©}(s) = 0 \\ s = +a: & w(s) = w^{©}(s) = 0 \end{cases} \quad (13)$$

From Eqs. (12), (13), natural frequencies and the corresponding vibrating shapes of the beam resonator can be obtained.

4 Calculations and Simulations

In this work, the main investigation is the detailed vibration shape of the beam resonator simultaneously. The sensor is made of silicon, thus E =$1.3\text{x } 10^{11}$ Pa, $\rho = 2.33 \text{ x } 10^{3}$ kg/m3, and $\mu = 0.17$. Moreover, the total element number of the beam N is 19 for FEM calculations.

The half-length and thickness of the square diaphragm are A=1mm and H=0.1 mm, respectively. In addition, the width and thickness of the beam are b=50 μm and h=5μm.

Define, Δf(B, D, a) [hz] = Δf (P, B, D, a) –f (0, 0, 0, 0) as the variation of the basic natural frequency of the beam within (0, p), with the x-axis deviation B. y-axis deviation D and the angular deviation a relative to its ideal location.

Define β(B, D, a)=[Δf(B, D, a,) -Δf(0, 0, 0)]/Δf(0, 0, 0)] as the relative variation of the basic natural frequency variation of the beam within (0, P), with the x-axis deviation B. y-axis deviation D and the angular deviation a relative to its ideal location.

Table 1: *The relative variation β(B, D, 0) of the frequency variation of the beam.*

D μm	*B μm*			
	0	*2*	*4*	*6*
0	*0.001*	*0.001*	*0.001*	*0.001*
2	*0.002*	*0.001*	*0.001*	*0.001*
4	*0*	*0.001*	*0.001*	*0.001*
6	*0.001*	*0.001*	*0.001*	*0.001*

Table 2: *The relative variation β(B, D, 3) of the frequency variation of the beam.*

D μm	*B μm*			
	0	*2*	*4*	*6*
0	*0.002*	*0.002*	*0.001*	*0.001*
2	*0.001*	*0.001*	*0.002*	*0.002*
4	*0.001*	*0.001*	*0.001*	*0*
6	*0.001*	*0.001*	*0.001*	*0.001*

Table 3: *The relative variation β(B, D, -3) of the frequency variation of the beam.*

D μm	*B μm*			
	0	*2*	*4*	*6*
0	*0.001*	*0.002*	*0.001*	*0.001*
2	*0*	*0.002*	*0.001*	*0.001*
4	*0.001*	*0.002*	*0*	*0.001*
6	*0.002*	*0.001*	*0.002*	*0.001*

Table's 1~3 shows β(B, D, 0), (a= 0deg), β(B, D, 3) (a=+3deg) and β(B, D, -3) (a =-3deg.), within (0, 106)pa. as the beam is located at different positions, i. e., with different ,x-axis deviation B, y-axis deviation D and the angular deviation a relative to its ideal location on the square diaphragm. The design ideal location is (-300, +300) μm (or L=600μm) within the positive stress range of the beam, and the beam's axial direction is along the x- axis of the square diaphragm, which corresponds to B = 0, D=0, a=0. In addition, $f(0, 0, 0)$= 106648Hz. $\Delta f(0, 0, 0)$=9924Hz.

From Table's 1~3, the variation of the basic natural frequency of the beam, which is influenced by the deviation D, the deviation B, and the angular deviation a of the beam relative to its ideal location, are almost the same within the positive stress range.

Table's 4~6 shows β(B, D, 0), (a= 0deg), β(B, D, 3) (a=+3deg) and β(B, D, -3) (a =3deg.), within (0, 106)pa. as the beam is located at different positions, i. e., with different ,x-axis deviation B, y-axis deviation D and the angular deviation a relative to its ideal location on the square diaphragm. The design ideal location is (+700, +1000) μm (or L=200μm) within the negative stress range of the beam, and the beam's axial direction is along the x- axis of the square diaphragm, which corresponds to B = 0, D=0, a=0. In addition, $f(0, 0, 0)$= 426564Hz. $\Delta f(0, 0, 0)$=10475Hz.

Table 4: *The relative variation β(B, D, 0) of the frequency variation of the beam.*

D μm	*B μm*			
	0	*-2*	*-4*	*-6*
0	*0*	*-0.005*	*-0.019*	*-0.025*
2	*0*	*-0.006*	*-0.021*	*-0.025*
4	*0.001*	*-0.006*	*-0.018*	*-0.026*
6	*0.002*	*-0.005*	*-0.018*	*-0.025*

Table 5: *The relative variation β(B, D, 3) of the frequency variation of the beam.*

D μm	*B μm*			
	0	*-2*	*-4*	*-6*
0	*-0.001*	*-0.008*	*-0.021*	*-0.026*
2	*-0.001*	*-0.011*	*-0.021*	*-0.026*
4	*-0.001*	*-0.012*	*-0.017*	*-0.031*
6	*-0.002*	*-0.013*	*-0.023*	*-0.029*

Table 6: *The relative variation β(B, D, -3) of the frequency variation of the beam.*

D μm	*B μm*			
	0	*-2*	*-4*	*-6*
0	*-0.001*	*-0.008*	*-0.025*	*-0.030*
2	*-0.001*	*-0.012*	*-0.025*	*-0.030*
4	*-0.001*	*-0.012*	*-0.026*	*-0.030*
6	*-0.002*	*-0.010*	*-0.025*	*-0.033*

From Table's 1~3, the variation of the basic natural frequency of the beam, which is influenced by the deviation D, the deviation B, and the angular deviation a of the beam

relative to its ideal location, within the negative stress range. Therefore, the y-axis deviation B should be reduced as much as possible. Comparing the above tables, it is obvious that locating the beam in the middle of the square diaphragm is much better than at the edge.

5 Conclusion

Based on the Finite Element Method model and analyses of the initial stresses applied to the beam resonator attached to a square diaphragm, this paper first calculates, analyses and investigates the relationship between the basic natural frequency of the beam resonator and the measured pressure for two error models. An important result is obtained it is necessary to monitor the processing accuracy in the x-axis, y-axis and the reference angle a relative to the ideal coordinate, within the positive stress range, while only in the x-axis within the negative stress range as the beam axial direction is along the x-axis of the square diaphragm. In addition, locating the beam in the middle of the square diaphragm is much better than at the edge.

References

[1] Masayoshi Esashi. Resonant Sensors by Silicon Micromachining [C]. Proceedings of the Annual IEEE International Frequency Control Symposium, 1996: 609-614.

[2] M. P. Henry, D. W. Clarke, N. Archer, etc. A self-validating digital Coriolis mass_flow meter: an overview [J]. Control Engineering Practice 8, 2000: 487-506.

[3] M.V Shutov, D L Howard, E E Sandoz, Electrostatic actuators with long range translation,, the 12th International Conference on Solid-State Sensors, Actuators and Microsystems, 1: 356-359(2003).

[4] Brian D Jensen, Senol Mutlu, Sam Miller, Shaped comb fingers for tailored electromechanical restoring force, Journal of Microelectromechanical Systems, 12（3）: 373-383(2003).

[5] Middelhock S. Quo vadis silicon sensor[J]. Sensor and Actuators, 1994, A41/42: 1-8.

[6] Luo R C. Sensor technologies and microsensor issues for mechatronics systems (Invited Paper)[J]. IEEE/ASME Transactions on Mechatronics, 1996, 1(1): 39-49.

[7] Parsons P, Glendinning A, Angelidis D. Resonator sensor for high accuracy pressure measurement using silicon technology[M]. IEEE Aerospace Electronic Systems, 1992, 7(7): 45-48.

[8] Buser R A, Derooij N F. Resonant silicon structures[J]. Sensors and Actuators, 1989, A17, 145-154.

[9] Zook J D, Burns D W. Characteristics of polysilicon resonant microbeams[J].Sensors & Actuators, 1992, A 35: 51-59.

[10] Zhang L M, Uttamchandani D, Culshaw B. Measurement of the mechanical properties of silicon microresonantors[J]. Sensors & Actuators, 1991, A 29: 79-84.

[11] Buser Rudolf A, de Rooij Nicolaas F, Silicon pressure sensor based on a resonating element[J]. Sensors & Actuators, 1991, A 25-27 : 717-722.